



Highly Efficient Removal of Uranium(VI) From Aqueous Solution Using the Polyethyleneimine Modified Magnetic Chitosan

Zhihui Wang¹ · Yanfei Wang¹ · Chen Yao¹

Accepted: 12 July 2021 / Published online: 20 July 2021

© The Author(s), under exclusive licence to Springer Science+Business Media, LLC, part of Springer Nature 2021

Abstract

In this study, Polyethyleneimine modified magnetic chitosan (MCS-PEI) was synthesized by grafting polyethyleneimine onto chitosan and adding magnetic Fe_3O_4 with sodium polyphosphate as crosslinking agent. The structure of the prepared material was characterized by FT-IR, SEM, EDS, XRD and XPS, which showed MCS-PEI was successfully synthesized. After a series of single factor experiments, the adsorption data fitted well with the Langmuir model ($R^2=0.99$), being the maximum adsorption capacity equal 181.8 mg g^{-1} . The pseudo-second-order model ($R^2=0.997$) and Dubinin-Radushkevich model ($R^2=0.9598$) indicated that the adsorption process was chemical adsorption. And thermodynamic studies showed that the adsorption was spontaneous and exothermic. The adsorption rate decreased by no more than 4% after the four adsorption–desorption experiments. This work illustrates that MCS-PEI is an environmental friendly, efficient and low-cost adsorbent.

Keywords Polyethyleneimine · Magnetic chitosan · Adsorption · Uranium(VI)

Introduction

Currently, nuclear energy plays an irreplaceable role in mitigating climate warming because of its high energy density and environmental friendliness [1–4]. So it is one of the important energy sources to solve the problem of the world's power shortfalls. But large amounts of radioactive waste are released from mineral mining, reprocessing of spent nuclear fuels, and other related activities [1, 5–7]. Although uranium is one of the important raw materials for the nuclear energy industry, it is the kind of long-lived and highly toxic radioactive pollutant with the characteristics of persistence and biological accumulation [3, 5, 8–12]. Uranium exists in the form of uranium(VI) [13]. If the uranium(VI) solution is not strictly managed, it will eventually accumulate in the human body, causing varying degrees of damage to the kidney, lung and nervous system [4, 14–20]. So, it can lead to having serious negative impacts on the ecosystem and human health [8, 10, 21–24].

Compared with ion-exchange [25], chemical precipitation [26] and solvent extraction [14], adsorption is considered to be the most effective and economical technique with simplicity and flexibility for removing uranium(VI) from aqueous solution [8, 19, 27]. And adsorbents may be more appropriate for the removal of metal ions owing to its cost-effective and simple process [28–31].

In recent years, biomaterials [such as chitosan (CS)] have attracted the attention of researchers in the field of environmental remediation because of its low cost and easy availability. CS is a kind of multifunctional polymer material which has no toxicity, harmlessness and high affinity, and has porous structure and degradable properties [5, 19, 32, 33]. It can adsorb uranium(VI) from aqueous solution because CS has abundant adsorption sites [34, 35]. Therefore, CS is considered to be one of the most suitable natural polymer materials for separation and biomedical technology. However, the poor mechanical properties of CS make it difficult to recover, and the adsorption capacity of chitosan for uranium(VI) is poor, which limit the application of it [36, 37–39]. At present, polyethyleneimine (PEI) is often used in dye adsorption, but it is rarely used in the adsorption of radioactive materials [26, 39–42]. It was found that the grafting of PEI onto CS increased the number of amino groups and improved the adsorption performance [38, 39]. By adding magnetic nanometer Fe_3O_4 to CS, the adsorbents

✉ Yanfei Wang
wyf_hn@hotmail.com

¹ School of Chemistry and Chemical Engineering,
University of South China, Hengyang 421001,
People's Republic of China

were easily separated from aqueous solution by the magnetic response [37]. Therefore, it is feasible to modify magnetic CS with PEI using sodium polyphosphate as crosslinking agent.

In this work, firstly, the MCS-PEI was synthesized by precipitation polymerization. Secondly, the structure and composition of the MCS-PEI were characterized. Next, the adsorption conditions were optimized by single factor experiments to study the adsorption mechanism. Finally, by comparing the existing adsorbents, the advantages of the adsorbent with high adsorption efficiency and high economic and environmental benefit were highlighted. It is helpful to expand the application of CS in the field of environmental protection.

Experiment

Main Materials

CS ($\geq 95\%$ deacetylation) and PEI were purchased from Shanghai Aladdin Biochemical Technology Co., Ltd. (Shanghai, China). Sodium polyphosphate was purchased from Shijiazhuang Donghua Chemical Co., Ltd. FeSO_4 and FeCl_3 were purchased from Tianjin Fuchen Chemical Reagent Co., Ltd and Taishan chemical plant, Guangdong Province, respectively. $\text{UO}_2(\text{NO}_3)_2 \cdot 6\text{H}_2\text{O}$ was purchased from a commercial supplier. The reagents used were AR. Preparation of $1.00 \text{ g} \cdot \text{L}^{-1}$ uranium(VI) solution: 0.186 g $\text{UO}_2(\text{NO}_3)_2 \cdot 6\text{H}_2\text{O}$ was diluted to 100 mL with deionized water. Preparation of Arsenazo III solution: 0.1250 g of Arsenazo III was diluted to 250 mL with deionized water. Sodium acetate-chloroacetic acid buffer with pH 2.5 was prepared [21, 26].

Preparation of the Fe_3O_4

The FeSO_4 and FeCl_3 were dissolved in 100 mL distilled water and stirred for 60 min at 323.15 K in the nitrogen atmosphere. Then the pH of solution was adjusted to 10 by dropping $\text{NH}_3 \cdot \text{H}_2\text{O}$. And the mixture solution was stirred for 3 h at 363.15 K . The precipitate was washed to neutral with distilled water and dried in the vacuum.

Preparation of the MCS-PEI

1 g of CS was dissolved in 100 mL of 2% CH_3COOH solution and 2 g of sodium polyphosphate was added. The mixture solution was heated at 328.15 K . Then 10 mL of 0.1 M $\text{Ce}(\text{NH}_4)_2(\text{NO}_3)_6$ was added, and the reaction time was 10 min . 4 g of PEI was added and the mixture was then cooled at 298.15 K for 5 h under stirring. When 0.5 g of Fe_3O_4 was added, the pH of the solution was adjusted

between 7 and 8. After stirring for 2 h and ultrasonic for 1 h . After the reaction, the products were magnetically separated and rinsed with deionized water until pH was 7, and finally freeze-dried for a night. The sample was denoted as MCS-PEI. The synthetic route of MCS-PEI was shown in Fig. 1. It was also shown in Fig. 1 that the adsorbent had good magnetism.

Adsorption Experiments

The effects of significant parameters on adsorption including temperature, pH, adsorbent dosage, initial concentration and time were studied by a series of experiments. The mass ($0.003\text{--}0.008 \text{ g}$) of MCS-PEI was added to 20 mL of uranium(VI) solution ($10\text{--}60 \text{ mg} \cdot \text{L}^{-1}$). The pH was adjusted to $3.0\text{--}8.0$. Then the conical flask was oscillated on the thermostatic water bath oscillator for 30 min to 240 min at the set temperature ($298.15\text{--}323.15 \text{ K}$). After the oscillation, the solid–liquid separation was carried out using the ultrafiltration membrane. The concentration of uranium(VI) was measured by ultraviolet–visible spectrophotometry (UV-2100) at 650 nm . The concentration of uranium(VI) was determined by a standard curve. The fitted linear equation was $y = 0.0171x + 0.0124$ (x ($\text{mg} \cdot \text{L}^{-1}$) was the concentration of uranium(VI) and y was the absorbance; $R^2 = 0.9992$) [26, 27]. The adsorbents loaded with uranium(VI) were desorbed by mixing with 20 mL 0.1 M NaOH. After desorption for 4 h , uranium(VI) was subjected to a continuous adsorption–desorption cycle using the same adsorbent to evaluate the reusability.

The adsorption capacity (Q , $\text{mg} \cdot \text{g}^{-1}$) and the removal efficiency (R , %) were calculated according to the following equations:

$$Q = C_0 - C_V / m \times V \quad (1)$$

$$R(\%) = C_0 - C_V / C_0 \times 100 \quad (2)$$

m and V represented the weight (g) of the MCS-PEI and the volume (L) of the solution, respectively. C_0 and C_V were the initial and equilibrium uranium(VI) concentration ($\text{mg} \cdot \text{L}^{-1}$), respectively.

Results and Discussion

Characterization Research

The MCS-PEI was characterized and the mechanism of uranium(VI) adsorption was explored. Figure 2 showed the FT-IR spectra of CS and MCS-PEI. Figure 2a showed the FT-IR spectra of CS, in which the wide peak at 3423 cm^{-1} was attributed to the overlap of the stretching vibration of

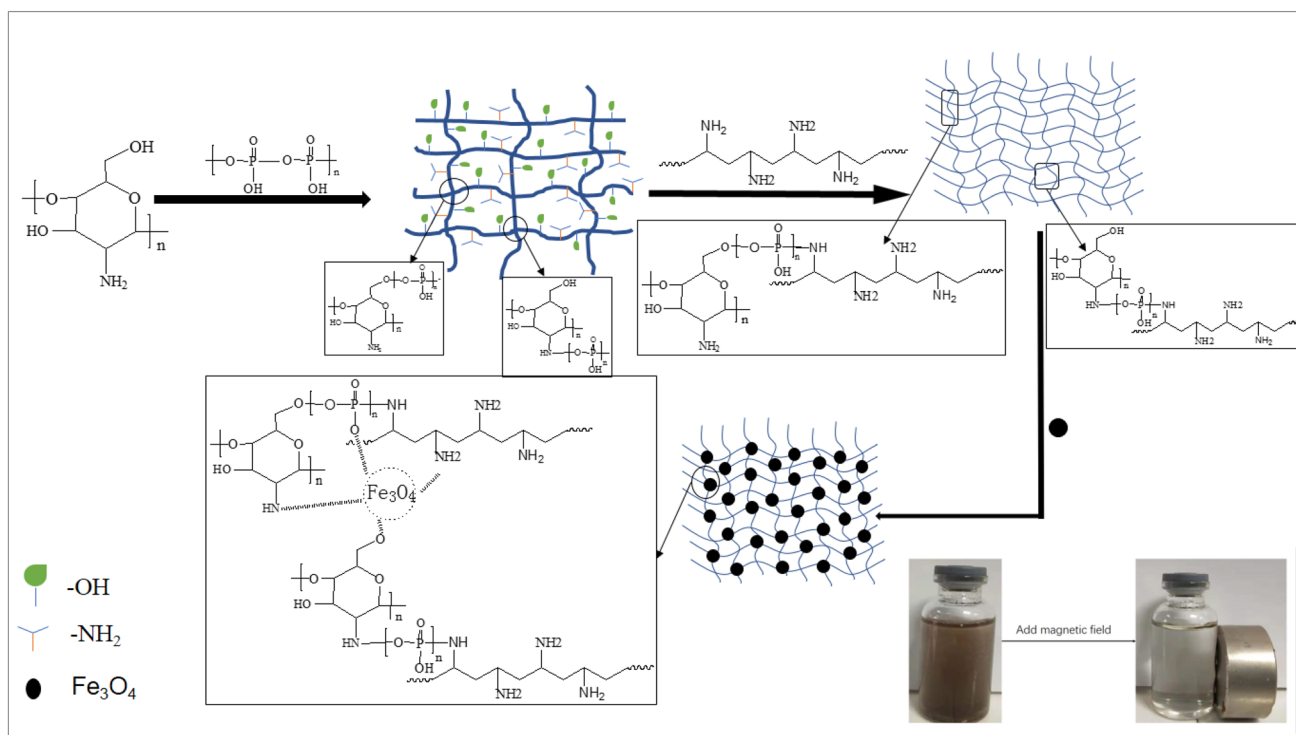


Fig. 1 The synthetic route of the MCS-PEI

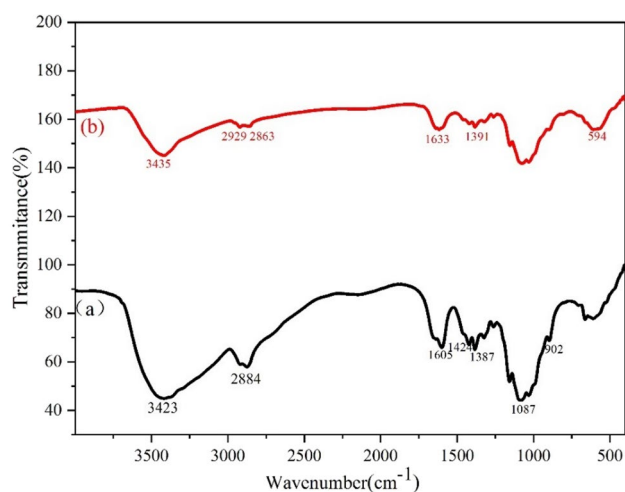


Fig. 2 The FT-IR spectra of different monomers: (a) CS and (b) MCS-PEI

–OH and –NH₂. There was a stretching vibration peak of –CH at 2884 cm⁻¹. The bending vibration peak of 1605 and 1424 cm⁻¹ were caused by the –NH₂. The bending vibration peak at 1387 cm⁻¹ belonged to the –CH. The stretching vibration of C–O at C₃ was a strong and sharp adsorption band at 1087 cm⁻¹. Also, the peak at 902 cm⁻¹ belonged to a pyridine ring stretch [40]. Figure 2b showed the FT-IR of MCS-PEI. It was found that the peaks in Fig. 2a were

roughly similar to those in Fig. 2b. And a new peak appeared at 594 cm⁻¹, which was related to the vibration peak of Fe–O of Fe₃O₄ [41]. Besides, the peak strength of 1424 and 1387 cm⁻¹ decreased, which might be caused by the crosslinking of –NH₂ and sodium polyphosphate. The peak values of 3435 and 1633 cm⁻¹ were higher and the intensity was higher, indicating that the number of –NH₂ was increasing. In addition, Compared with the FT-IR spectrum of CS, the symmetric and asymmetric stretching vibration peaks of PEI at 2929 and 2863 cm⁻¹ showed that PEI was successfully grafted onto CS [42].

The MCS-PEI was characterized by SEM. The image before adsorption was shown in Fig. 3a. It was obvious that there was a large void structure in MCS-PEI, which was due to the irregular shape of the cross-linking among the components of MCS-PEI. These pore structures exposed the adsorption sites of MCS-PEI, resulting in the chelation between uranium(VI) and functional groups, thus improving the adsorption performance [41, 42]. After adsorption of uranium(VI), the pore structure became smaller, as shown in Fig. 3b, which indicated that uranium(VI) was adsorbed on MCS-PEI. EDX is a tool for studying the constituent elements of material. The presence of Fe and P elements confirmed that sodium polyphosphate and Fe₃O₄ were involved in the synthesis of MCS-PEI, and further confirmed the above reasons. As shown in Fig. 4b, the presence of U

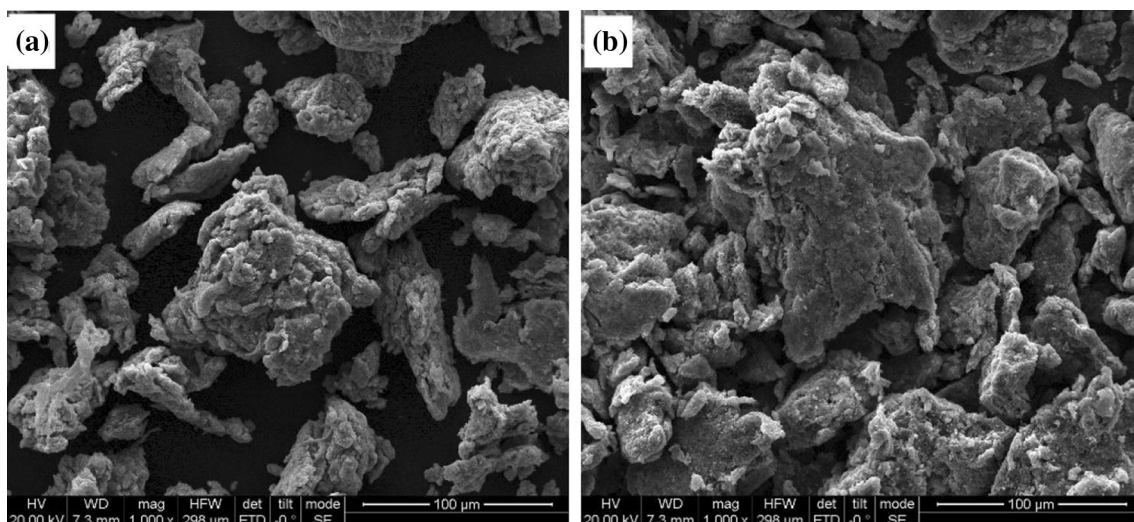


Fig. 3 The SEM of the MCS-PEI before (a) and after (b) loaded with uranium(VI)

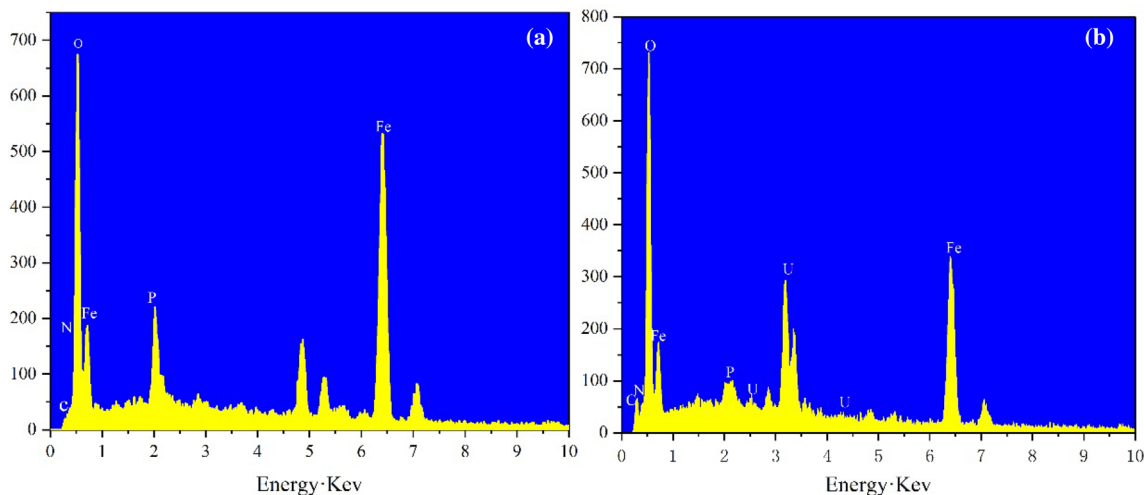


Fig. 4 EDS spectrums of the MCS-PEI before (a) and after (b) the adsorption of uranium(VI)

element indicated that MCS-PEI had adsorption effect on uranium(VI).

The crystal structure of MCS-PEI was studied by XRD, and the characterization results are shown in Fig. 5. It could be seen that the typical diffraction peaks (220, 311, 400, 440 and 511) of Fe_3O_4 all appear in the XRD patterns, which indicated that the structure of Fe_3O_4 was well preserved throughout the fabrication process [26, 39, 41]. At $2\theta=20.3^\circ$ There was a peak corresponding to the amorphous phase of CS, but in the XRD pattern of MCS-PEI, the peak became smaller and wider, which might be caused by the grafting of PEI and CS. These results confirmed that Fe_3O_4 was coated in MCS-PEI [40, 42].

To further explain the adsorption mechanism of uranium(VI), XPS was used to further study the chemical bond morphology of the MCS-PEI surface, and the functional groups involved in the immobilization of uranium(VI) were inferred. As expected, a new uranium peak, namely U 4f peak, was found on XPS of the adsorbed sample [23]. In addition, it could be seen in Fig. 6 that the intensity of the high-resolution N 1 s spectra also changed significantly before and after the adsorption of uranium(VI). N 1 s has two peaks before adsorption, representing amino group. However, the binding energy of N changed from 400.7 to 401.5 eV after adsorption. This might be due to the chelation between uranium(VI) and amino group, which changed the environment around the electron, resulting in the increase of

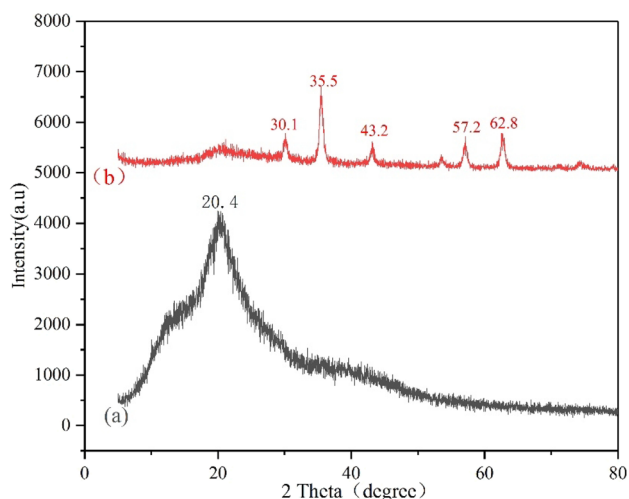


Fig. 5 XRD patterns of the CS (a) and the MCS-PEI (b)

binding energy [6, 17, 21, 27]. It indicated that the adsorption of uranium(VI) could not be separated from amino group.

Adsorption Experiment

Effect of pH

The pH is the key factor affecting the adsorption stability. Because it affects the form of uranium(VI) in solution and the surface potential of adsorbent surface. The results were shown in Fig. 7. With the increase of pH, the adsorption capacity first increased and then decreased. This was because the lower the pH was, the higher the protonation degree of amino group on MCS-PEI was, which was inferior to H^+ . At the same time, the electrostatic repulsion of H^+ also prevented uranium(VI) from approaching the active center of the adsorbent, resulting in the decrease of adsorption of uranium(VI) by MCS-PEI [1, 12, 31]. The positive

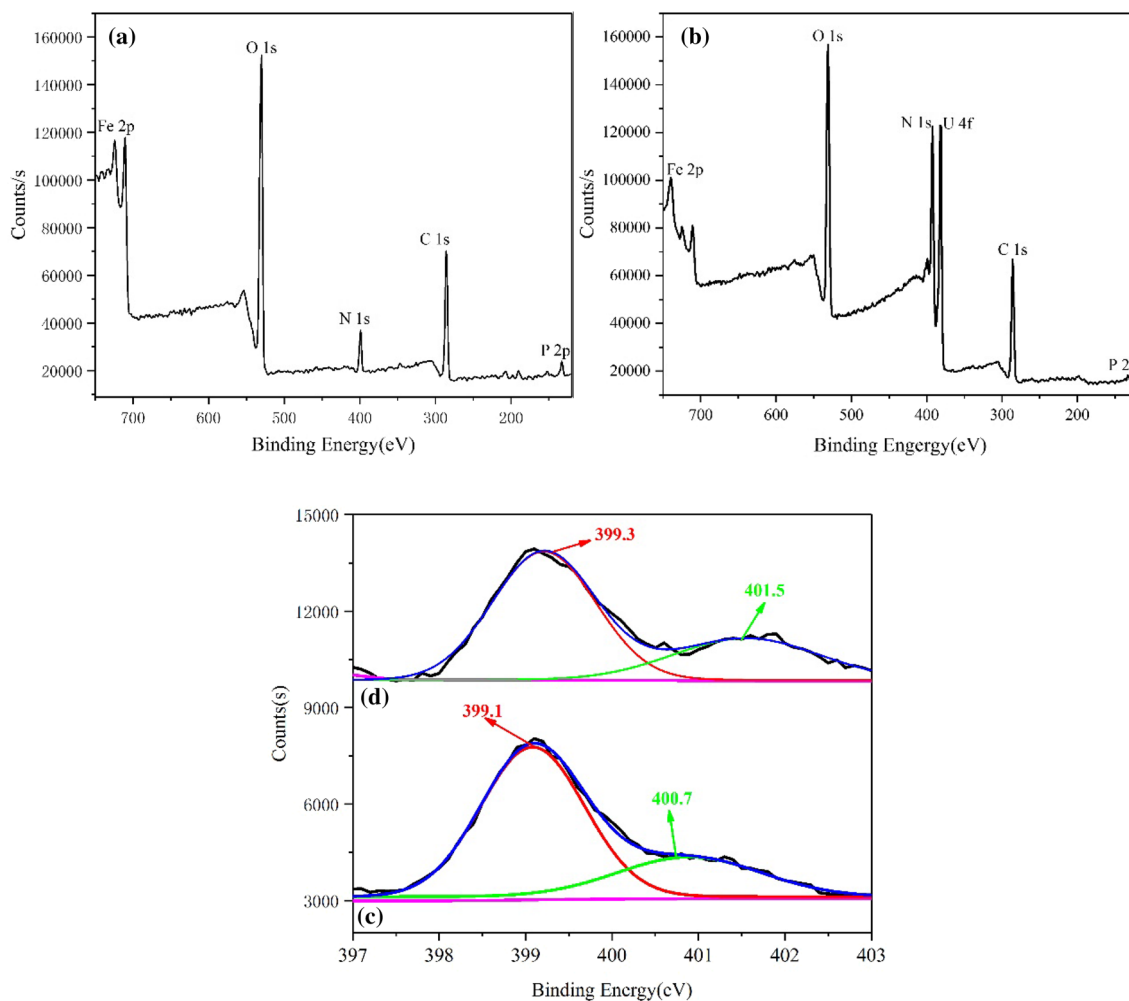


Fig. 6 Wide XPS spectra of the MCS-PEI before (a) and after (b) the adsorption of uranium(VI); N 1 s narrow XPS spectra of before (c) and after (d) the adsorption of uranium(VI)

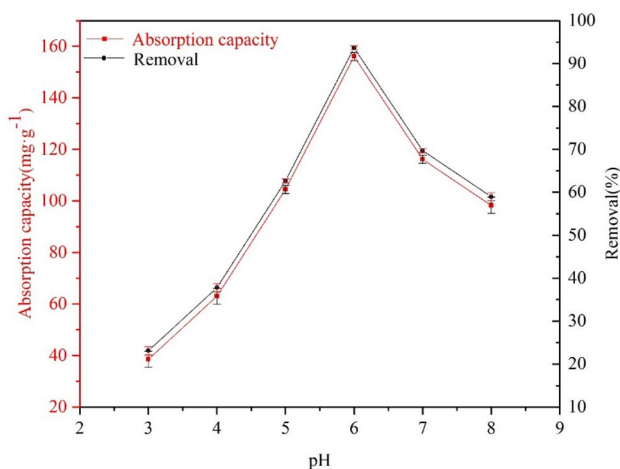


Fig. 7 The effect of initial pH on adsorption of uranium(VI) (initial uranium(VI) concentration 50 mg·L⁻¹, the aqueous volume 20 mL, temperature 298.15 K, the adsorbent weight 0.006 g, contact time 180 min)

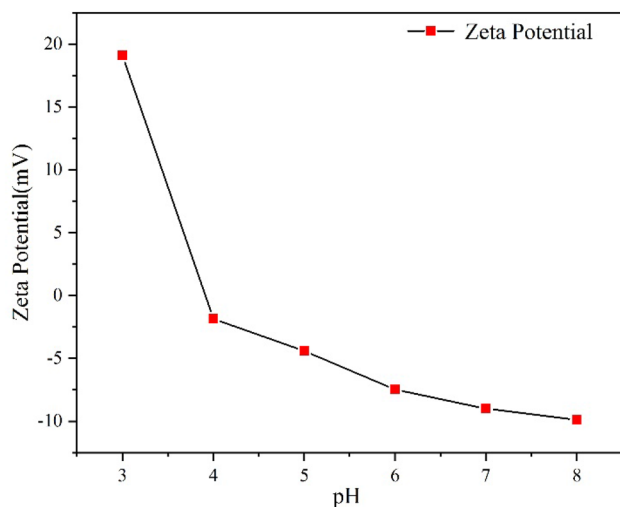


Fig. 8 The zeta potential of MCS-PEI

and negative charges on the adsorbent surface could effectively explain this phenomenon, as shown in Fig. 8. In addition, Fe₃O₄ was unstable in high acid environment and easy to be destroyed, resulting in loss of magnetism. When pH value exceeded 6.0, complex anions such as (UO₂)₃(OH)₇⁻, UO₂(OH)₃⁻, UO₂(CO₃)₃⁴⁻ and UO₂(CO₃)₂²⁻, might be formed on the surface of MCS-PEI, which increased the electrostatic repulsion and decreased the adsorption efficiency [3, 21, 26, 27]. Therefore, in the following study, the pH of uranium(VI) concentration was 6.0.

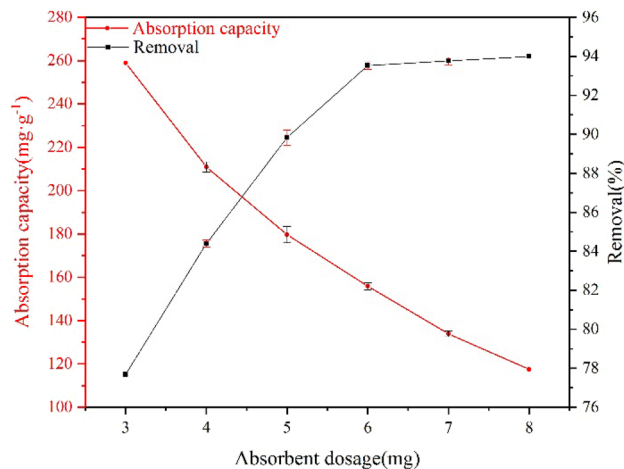


Fig. 9 The effect of adsorbent dosage on adsorption of uranium(VI) (initial uranium(VI) concentration of 50 mg·L⁻¹, pH 6.0, the aqueous volume 20 mL, temperature 298.15 K, contact time 180 min)

Effect of Adsorbent Dosage

The adsorbent dosage is another important parameter affecting the adsorption process. The experimental results were shown in Fig. 9. With the increase of the dosage, the removal rate of uranium(VI) increased first and then tended to be stable. This might be due to the increase of effective adsorption sites with the increase of adsorbent dosage, which reduced the amount of uranium(VI) in aqueous solution. At the same time, because the amount of uranium(VI) in the solution is certain, the removal rate tended to be stable gradually. However, the adsorption capacity decreased with the increase of adsorbent dosage, because the adsorption capacity decreased with the decrease of uranium(VI) amount in unit mass.

Effect of Contact Time and Kinetics Study

This study investigated the effect of adsorption time on the adsorption of MCS-PEI, and the results were shown in Fig. 10. The adsorption of uranium(VI) reached equilibrium within 180 min and remained stable during the remainder of contact time. Uranium(VI) first diffused to the surface of the adsorbent and then allowed uranium(VI) to enter into the adsorbent through a network structure. Uranium(VI) was adsorbed by the active sites until the sites were occupied, so the adsorption rate became very slow until equilibrium was reached.

To evaluate the adsorption capacity of the adsorbents on uranium(VI) at adsorption equilibrium, two adsorption kinetic models were established and studied respectively.

Pseudo-first-order model:

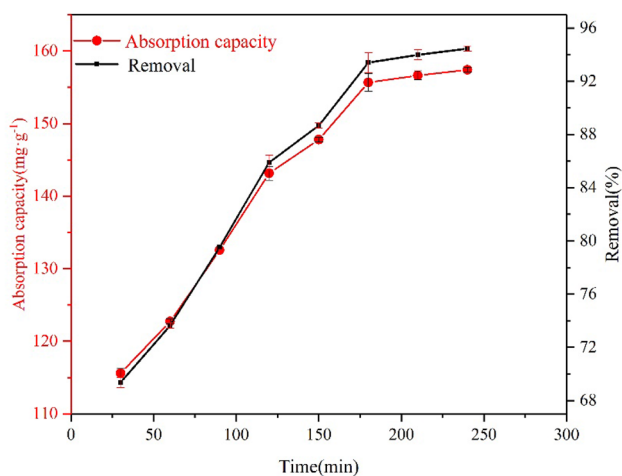


Fig. 10 The effect of contact time on adsorption of uranium(VI) (initial uranium(VI) concentration of 50 mg L⁻¹, pH 6.0, the aqueous volume 20 mL, temperature 298.15 K, adsorbent weight 0.006 g)

$$\ln(Q_e - Q_t) = \ln Q_e - K_1 \cdot t \tag{3}$$

Pseudo-second-order model:

$$t/Q_t = 1/K_2 \cdot 1/(Q_e)^2 + 1/Q_e \cdot t \tag{4}$$

where Q_e and Q_t represented the adsorption capacity (mg·g⁻¹) of the adsorbents at equilibrium and at any time, respectively. K_1 (min⁻¹) and K_2 (g·mg⁻¹·min⁻¹) represented the pseudo-first-order and pseudo-second-order model constants, respectively.

The adsorption kinetics of uranium(VI) by the MCS-PEI was illustrated in Fig. 11 at C_0 50 mg·L⁻¹. Compared with the pseudo-first-order model, the pseudo-second-order model was more suitable for fitting normal dynamics with

Table 1 Kinetic parameters for the adsorption

Kinetic parameters	Value
$Q_{e,exp}$ (mg·g ⁻¹)	156.7
Pseudo-first-order	
Q_e (mg·g ⁻¹)	141.2
K_1 (min ⁻¹)	0.0226
$\sqrt{R^2}$	0.90224
Pseudo-second-order	
Q_e (mg·g ⁻¹)	169.5
K_2 (min ⁻¹)	0.00028
R^2	0.997

the correlation coefficient (R^2) larger than 0.997, which suggested that the interactions of uranium(VI) and surfaces rather than mass transport were the rate-determining steps of adsorption, so the uranium(VI) adsorption process was mainly controlled by chemisorption in Table 1.

Effect of Initial Concentration and Isothermal Adsorption Study

To study the adsorption capacity of the prepared material, the influence of initial uranium(VI) concentration on the adsorption removal rate was studied. The results were shown in Fig. 12. With the increase of initial uranium(VI) concentration, the removal rate of uranium(VI) decreased. This was because as the initial uranium(VI) concentration in the aqueous solution increased, the mass of the uranium(VI) in the system increased, but the mass of the adsorbent remained the same. On the other hand, due to the high mobility of uranium(VI) in dilute solution, the interaction between uranium(VI) and adsorbents was also increased.

To study the maximum adsorption capacity of the adsorbent to uranium(VI), the adsorption isotherms with different

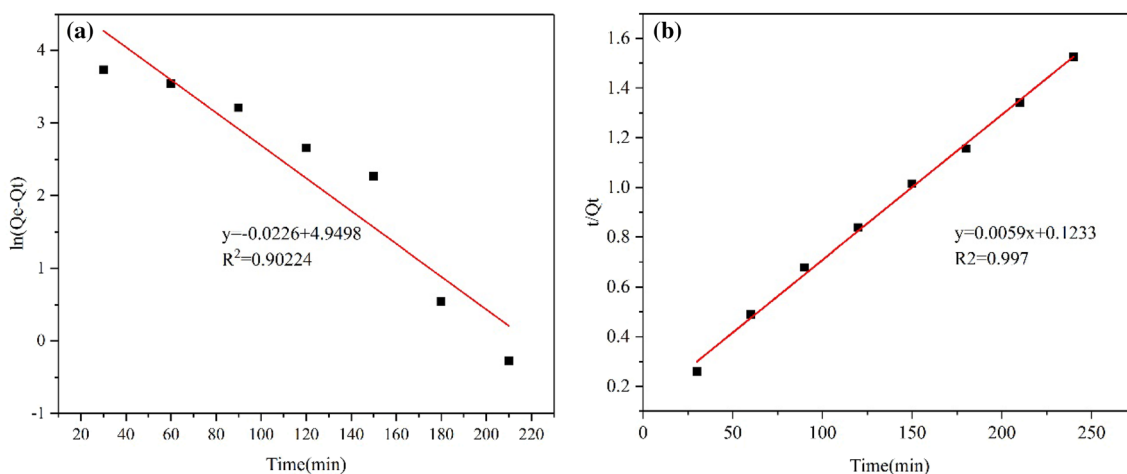


Fig. 11 Adsorption kinetics: pseudo-first-order (a) and pseudo-second-order (b) for adsorption of uranium(VI)

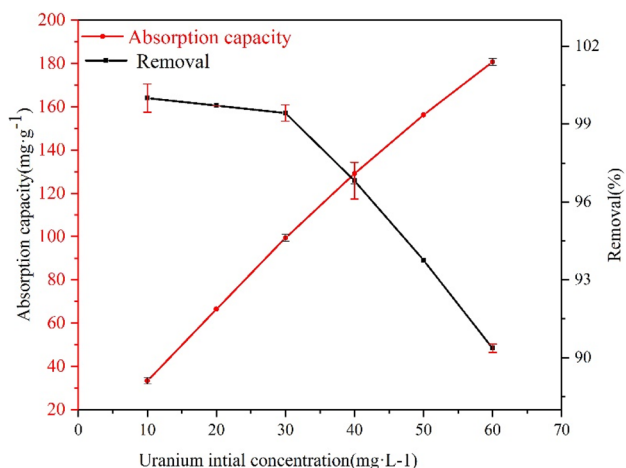


Fig. 12 The effect of initial concentration on adsorption of uranium(VI) (pH 6.0, the aqueous volume 20 mL, temperature 298.15 K, the adsorbent weight 0.006 g, contact time 180 min)

initial concentrations were tested at 298.15 K. Langmuir, Freundlich and Dubinin-Radushkevich (D-R) model were used to analyze the adsorption isotherm [43–45].

Langmuir model:

$$C_e/Q_e = C_e/Q_{\max} + 1/(K_L Q_{\max}) \quad (5)$$

The essential characteristics of the Langmuir model could be explained by the dimensionless equilibrium parameter R_L , which could be expressed by the following equation:

$$R_L = 1/(1 + C_0 \cdot K_L) \quad (6)$$

R_L value represented: adverse adsorption ($R_L > 1$), linear adsorption ($R_L = 1$), favorable adsorption ($0 < R_L < 1$) or irreversible adsorption ($R_L = 0$).

Freundlich model:

$$\ln Q_e = \ln K_F + \ln C_e/n \quad (7)$$

The D–R model is related to the adsorption energy. We can use the E_{DR} value of the isotherm to propose the adsorption mechanism of chemical adsorption or physical adsorption. When the E_{DR} value is between 8 and 16 $\text{kJ} \cdot \text{mol}^{-1}$, chemical reaction takes place in the adsorption process. When the E_{DR} value is less than 8 $\text{kJ} \cdot \text{mol}^{-1}$, the adsorption process takes place in a physical way.

D-R model:

$$\varepsilon = RT \ln \left(1 + \frac{1}{C_e} \right) \quad (9)$$

$$\ln Q_e = \ln X_{DR} - k_{DR} \varepsilon^2 \quad (10)$$

$$E_{DR} = (2k_{DR})^{-0.5} \quad (11)$$

Among them, Q_e ($\text{mg} \cdot \text{g}^{-1}$) represented the adsorption capacity at adsorption equilibrium, and C_e ($\text{mg} \cdot \text{L}^{-1}$) represented the concentration of uranium(VI) at adsorption equilibrium. Q_{\max} ($\text{mg} \cdot \text{g}^{-1}$) referred to the maximum adsorption capacity of adsorbents. K_L ($\text{L} \cdot \text{mg}^{-1}$) and K_F referred to the adsorption equilibrium constant of the Langmuir model and Freundlich model, respectively. And n was the Freundlich model constant related to adsorption strength. ε represented polanyi potential. X_{DR} represented D-R adsorption capacity ($\text{mol} \cdot \text{K} \cdot \text{g}^{-1}$). k_{DR} represented D-R constant related to the sorption energy ($\text{mol}^2 \cdot \text{K} \cdot \text{J}^{-2}$). R represented ideal gas constant ($8.314 \text{ J} \cdot \text{mol}^{-1} \cdot \text{K}^{-1}$) and T represented absolute temperature. E_{DR} represented free energy change ($\text{kJ} \cdot \text{mol}^{-1}$).

The data showed that R_L values ranged from 0 to 1 and n was between 1 to 10, which illustrated that the MCS-PEI was feasible to adsorb uranium(VI) in Table 2. The data presented in Table 3 showed that the Langmuir model ($R^2 = 0.99$) was more accurate than the Freundlich model ($R^2 = 0.97$) and the D-R model ($R^2 = 0.96$) for uranium(VI) adsorption, indicating that adsorption was monolayer adsorption Table 3. And the adsorption energy, E_{DR} value, was in the range of 8–16 $\text{kJ} \cdot \text{mol}^{-1}$. Therefore, the adsorption of uranium(VI) by MCS-PEI was controlled by chemical adsorption in Fig. 13.

Adsorption Thermodynamics

To further evaluate the effect of temperature on adsorption, the thermodynamic parameters of uranium(VI) adsorption were calculated by using the following equation. The adsorption thermodynamics of ΔG^0 , ΔS^0 and ΔH^0 were illustrated. The isotherms of adsorbents at different temperatures were shown in Fig. 14. The calculated parameters were shown in Table 4.

$$K_d = (C_0 - C_e)/C_e \cdot V/m \quad (8)$$

$$\ln K_d = \Delta S^0/R - \Delta H^0/(R \times T) \quad (9)$$

Table 2 Equilibrium parameters, R_L

Temperature 298.15 (K)	Uranium concentration ($\text{mg} \cdot \text{L}^{-1}$)					
	10	20	30	40	50	60
R_L	0.156	0.0844	0.0579	0.0441	0.0356	0.0298

Table 3 The isothermal adsorption model parameters

Isothermal parameters	Value
Langmuir isotherm	
Q_{max} (mg·g ⁻¹)	181.8
K_L (L·mg ⁻¹)	5
R^2	0.99
Freundlich isotherm	
K_f ((mg·g ⁻¹)/(mg·L ⁻¹) ^{1/n})	126.4
n	5.00
R^2	0.97058
D-R isotherm	
X_{DR}	249.64
$-k_{DR} \times 10^9$	3.40
R^2	0.9598
E_{DR} (kJ·mol ⁻¹)	12.12

Among them, K_d represented the equilibrium distribution coefficient of the adsorbent; C_0 and C_e were the initial and equilibrium concentrations of uranium(VI), respectively; V represented the solution volume; m represented the adsorbent dosage; T (K) represented the solution temperature; R (8.314 J mol⁻¹ K⁻¹) was the ideal gas constant; ΔH^0 (J mol⁻¹), ΔS^0 (J mol⁻¹ K⁻¹), ΔG^0 (J mol⁻¹) were the standard adsorption enthalpy, the standard adsorption entropy and Gibbs' free energy change of adsorption, respectively.

Based on the above isotherm findings, the thermodynamics governing the adsorption of uranium(VI) on adsorbents was examined. The results were shown in Table 4. The adsorption capacity decreased when the temperature increased, and ΔH^0 value was negative, indicating that the adsorption process was exothermic. The ΔG^0 value was negative, indicating that the adsorption process was spontaneous.

$$\Delta G^0 = \Delta H^0 - T \times \Delta S^0 \tag{10}$$

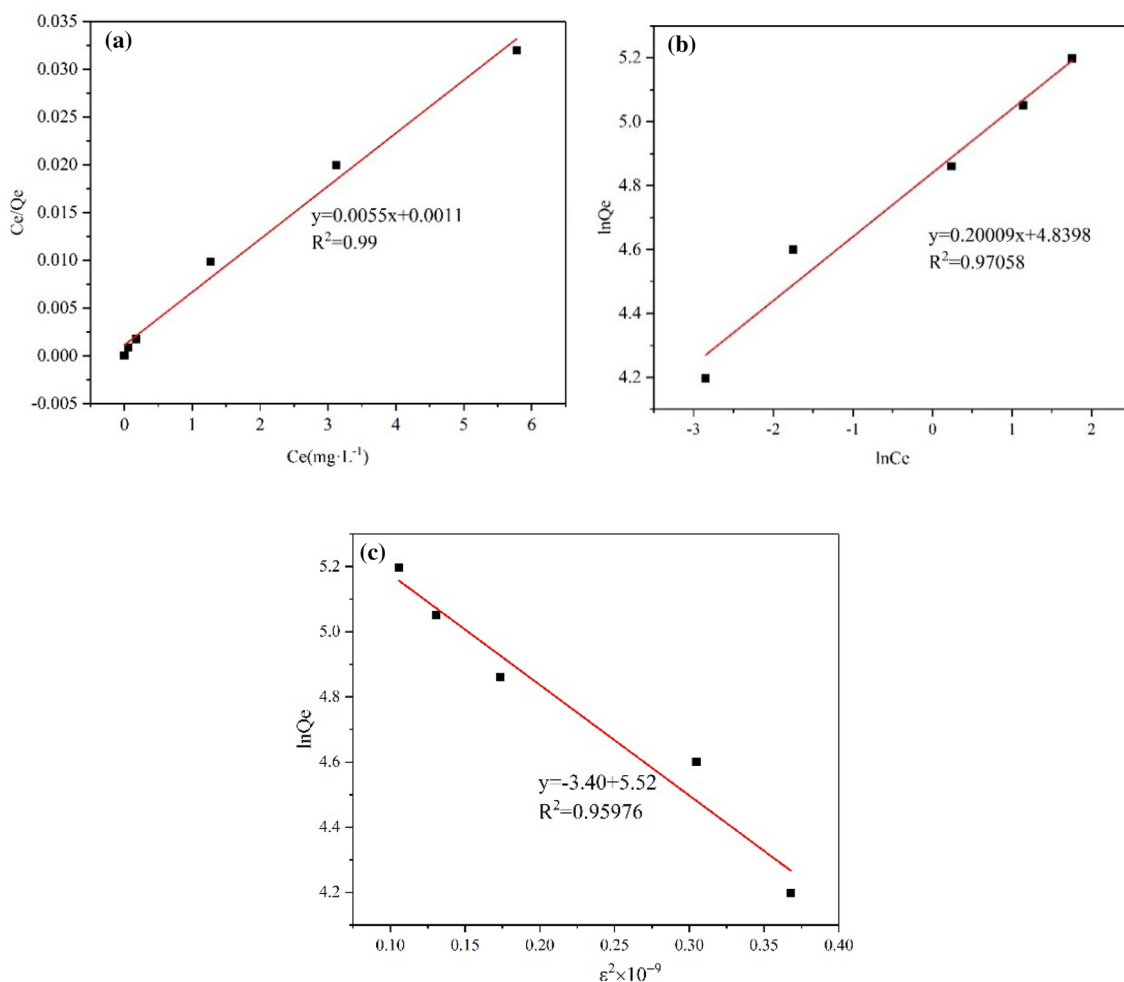


Fig. 13 Langmuir (a), Freundlich (b) and D-R (c) isotherm plot of uranium(VI) adsorption for the MCS-PEI

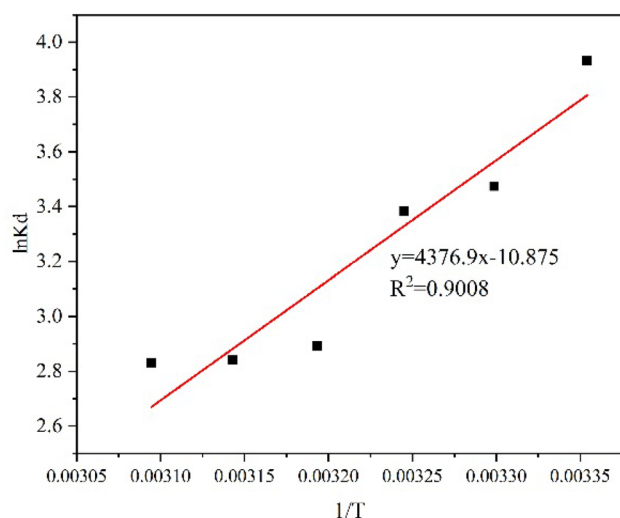


Fig. 14 The plot of the thermodynamic equation for the adsorption of uranium(VI) (initial uranium(VI) concentration of $50 \text{ mg}\cdot\text{L}^{-1}$, pH 6.0, the aqueous volume 20 mL, contact time 180 min, adsorbent weight 0.006 g)

Table 4 Thermodynamic parameter for uranium(VI) adsorption on MCS-PEI

T (K)	ΔG^0 (kJ·mol ⁻¹)	ΔH^0 (kJ·mol ⁻¹)	ΔS^0 (kJ·mol ⁻¹ ·K)
298.15	-9.43239	-36.3895	-0.09041
303.15	-8.98032		
308.15	-8.52824		
313.15	-8.07617		
318.15	-7.62409		
323.15	-7.17202		

Table 5 Recycling of MCS-PEI in the removal of uranium(VI)

Number of cycles	Initial uranium(VI) ($\text{mg}\cdot\text{L}^{-1}$)	Removal efficiency (%)
First cycle	50	93.8
Second cycle		93.2
Third cycle		91.1
Fourth cycle		89.8

Recyclability of the MCS-PEI

To demonstrate the recyclability of the MCS-PEI, 0.1 M NaOH was utilized to regenerate the MCS-PEI adsorbed

with $50 \text{ mg}\cdot\text{L}^{-1}$ of uranium(VI) at pH 6.0. As shown in Table 5, after four recycling uses, the removal efficiency of uranium(VI) decreases slightly from 93.8 to 89.8%, which was due to the inevitable mass loss of the adsorbent. As shown in Fig. 1, the magnetic effect could be used to recover the adsorbent to minimize the loss due to mass. It was very important for reducing the cost of actual uranium(VI) recovery applications.

Comparison With Different Adsorbents

In order to further predict the potential application prospect of the material, the experimental adsorption properties of various materials were compared. Table 6 showed the maximum adsorption capacity of modified chitosan adsorbent for uranium(VI). Compared with other adsorbents, the adsorption capacity of MCS-PEI was significantly higher than that of common adsorbents, and the use condition was mild and friendly to the environment [14]. Therefore, MCS-PEI is a low-cost and efficient adsorbent.

Conclusion

In this work, MCS-PEI with high adsorption capacity and environmental friendliness were synthesized by the precipitation polymerization. Through characterization, MCS-PEI was successfully synthesized and the amino group of MCS-PEI played a decisive role in the adsorption of uranium(VI). Under the optimized adsorption conditions, the adsorption capacity of the adsorbent was 156.7 mg g^{-1} and the removal rate was 93.8% at 298.15 K and pH 6.0. The pseudo-second-order model and Langmuir model could be well fitted to the adsorption process, indicating that the adsorption process was mainly affected by chemical adsorption. Thermodynamic analysis showed that the process was exothermic and spontaneous. In addition, MCS-PEI had excellent reusability and stability. Compared with other adsorbents, MCS-PEI was an environmental friendly, efficient and low-cost adsorbent. The results demonstrated that MCS-PEI was a promising adsorbent for the removal of radioactive pollutants from aqueous solution.

Acknowledgements This work was supported by the National Natural Science Foundation of China [51803088]; the Natural Science Foundation of Hunan Province, China [2020JJ5493]; and the Scientific Research Fund of Hunan Education Department [17C1360].

Author Contributions ZW: investigation, conceptualization, analysis, data curation, and writing—original draft; YW: resources, supervision, and writing—review; CY: writing—review and funding acquisition.

Table 6 Comparison of the uranium(VI) maximum adsorption capacities on MCS-PEI and other materials

Adsorbent	Adsorption capacity (mg·g ⁻¹)	pH	References
Chitosan/Fe ₃ O ₄ /SiO ₂ /2-phosphonobutane-1,2,4-tri-carboxylic acid	83.16	4.0	[6]
Chitosan/bentonite/acrylonitrile/3-hexenedinitrile	49.09	8.0	[13]
Chitosan/Fe ₃ O ₄ /cyclohexane/N-hexanol	187.26	5.0	[25]
Chitosan/Fe ₃ O ₄	42	5.0	[43]
Chitosan/Fe ₃ O ₄ /acrylo-nitrile/hydroxylamine hydro-chloride	117.65	6.0	[44]
Chitosan/epichlorohydrin	49.05	3.0	[45]
Chitosan/graphene oxide	50.51	5.0	[46]
Chitosan/FeS	92.45	4.16	[47]
Chitosan/carbon nanotubes	126.7	4.0	[48]
Chitosan/Fe ₃ O ₄ /polyethyleneimine/sodium polyphosphate	181.8	6.0	This study

Declarations

Conflict of interest The authors declare that they have no known competing financial interests or personal relationships that could have appeared to influence the work reported in this paper.

References

- Huang Z, Li Z, Wu Q, Zheng L, Min ZL, Chai Z, Wang X, Shi W (2018) Simultaneous elimination of cationic uranium(VI) and anionic rhenium(VII) by graphene oxide-poly(ethyleneimine) macrostructures: a batch, XPS, EXAFS, and DFT combined study. *Environ Sci Nano* 5(9):2077–2087
- Jiang C, Liu Y, Yuan D, Wang Y, Jia WC (2020) Investigation of the high U(VI) adsorption properties of phosphoric acid-functionalized heteroatoms-doped carbon materials. *Solid State Sci* 104:1293–2558
- Liu L, Yang W, Gu D, Zhao X, Pan Q (2019) In situ preparation of chitosan/ZIF-8 composite beads for highly efficient removal of U(VI). *Front Chem* 7:607
- Zhong X, Sun Y, Zhang Z, Dai Y, Wang Y, Liu Y, Hua R, Cao X, Liu Y (2019) A new hydrothermal cross-linking ion-imprinted chitosan for high-efficiency uranium removal. *J Radioanal Nucl Chem* 322(2):901–911
- Zhou L, Shang C, Liu Z, Huang G, Adesina AA (2020) Macroporous ion-imprinted chitosan foams for the selective biosorption of U(VI) from aqueous solution. *Int J Biol Macromol* 164:4155–4164
- Huang Y, Zheng H, Li H, Zhao C, Zhao R, Li S (2020) Highly selective uranium adsorption on 2-phosphonobutane-1,2,4-tricarboxylic acid-decorated chitosan-coated magnetic silica nanoparticles. *Chem Eng J* 388:124349
- Wang Y, Li Y, Li L, Kong F, Li W (2020) Preparation of three-dimensional fiber-network chitosan films for the efficient treatment of uranium contaminated effluents. *Water Sci Technol* 81(1):52–61
- Liu W, Zhang L, Chen F, Wang H, Wang Q, Liang K (2020) Efficiency and mechanism of adsorption of low-concentration uranium from water by a new chitosan/aluminum sludge composite aerogel. *Dalton Trans* 49(10):3209–3221
- Liu Y, Dai Y, Yuan D, Wang Y, Zou L (2017) The preparation of PZS-OH/CNT composite and its adsorption of U(VI) in aqueous solutions. *J Radioanal Nucl Chem* 314(3):1747–1757
- Liu Y, Ouyang Y, Huang D, Jiang C, Liu X, Wang Y, Dai Y, Yuan D, Chew JW (2020) N, P and S co-doped carbon materials derived from polyphosphazene for enhanced selective U(VI) adsorption. *Sci Total Environ* 706:136019
- Sun Z, Chen D, Chen B, Kong L, Su M (2018) Enhanced uranium(VI) adsorption by chitosan modified phosphate rock. *Colloids Surf A Physicochem Eng Aspects* 547:141–147
- Guo XJ, Chen RR, Liu Q, Liu JY, Yu J, Zhang HS, Li RM, Zhang ML, Wang J (2018) Superhydrophilic phosphate and amide functionalized magnetic adsorbent: a new combination of anti-biofouling and uranium extraction from seawater. *Environ Sci Nano* 5(10):2346–2356
- Anirudhan TS, Lekshmi GS, Shainy F (2018) Synthesis and characterization of amidoxime modified chitosan/bentonite composite for the adsorptive removal and recovery of uranium from seawater. *J Colloid Interface Sci* 534:248–261
- Guo X, Chen R, Liu Q, Liu J, Zhang H, Yu J, Li R, Zhang M, Wang J (2018) Superhydrophilic phosphate and amide functionalized magnetic adsorbent: a new combination of anti-biofouling and uranium extraction from seawater. *Environ Sci Nano* 5(10):2346–2356
- Lu W, Dai Z, Li L, Liu J, Wang S, Yang H, Cao C, Liu L, Chen T, Zhu B, Sun L, Chen L, Li H, Zhang P (2020) Preparation of composite hydrogel (PCG) and its adsorption performance for uranium(VI). *J Mol Liq* 303:112604
- Jiang X, Wang H, Hu E, Lei Z, Wang Q (2020) Efficient adsorption of uranium from aqueous solutions by microalgae based aerogel. *Microporous Mesoporous Mater* 305:110383
- He J, Jin J, Wang Z, Yin H, Wei C, Xu X (2018) Encapsulating nanosilica into polyacrylic acid and chitosan interpenetrating network hydrogel for preconcentration of uranium from aqueous solutions. *J Radioanal Nucl Chem* 317(3):1299–1309
- Liu Y, Zhao Z, Yuan D, Wang Y, Dai Y, Zhu Y, Wei Chew J (2018) Introduction of amino groups into polyphosphazene framework supported on CNT and coated Fe₃O₄ nanoparticles for enhanced selective U(VI) adsorption. *Appl Surf Sci*. <https://doi.org/10.1016/j.apsusc.2018.10.097>
- Rostamian R, Firouzzare M, Irandoust M (2019) Preparation and neutralization of forcespun chitosan nanofibers from shrimp shell waste and study on its uranium adsorption in aqueous media. *React Funct Polym* 143:104335
- Yi X, Xu Z, Liu Y, Guo X, Ou M, Xu X (2017) Highly efficient removal of uranium(VI) from wastewater by polyacrylic acid hydrogels. *RSC Adv* 7(11):6278–6287
- Ma Z, Wang Y, Luo Y, Xie X, Xiong Z (2020) Highly efficient elimination of thorium(IV) from aqueous solution using

- poly(cyclotriphosphazene-co-melamine) microspheres. *J Radioanal Nucl Chem* 323(2):993–1002
22. Mishima K, Du X, Miyamoto N, Kano N, Imaizumi H (2018) Experimental and theoretical studies on the adsorption mechanisms of uranium(VI) ions on chitosan. *J Funct Biomater* 9(3):49
 23. Li S, Yang P, Liu X, Zhang J, Xie W, Wang C, Liu C, Guo Z (2019) Graphene oxide based dopamine mussel-like cross-linked polyethylene imine nanocomposite coating with enhanced hexavalent uranium adsorption. *J Mater Chem A* 7(28):16902–16911
 24. Sureshkumar MK, Das D, Mallia MB, Gupta PC (2010) Adsorption of uranium from aqueous solution using chitosan-tripolyphosphate (CTPP) beads. *J Hazard Mater* 184(1–3):65–72
 25. Zhou L, Shang C, Liu Z, Huang G, Adesina AA (2012) Selective adsorption of uranium(VI) from aqueous solutions using the ion-imprinted magnetic chitosan resins. *J Colloid Interface* 366(1):165–172
 26. Xie X, Wang Y, Xiong Z, Li H, Yao C (2020) Highly efficient removal of uranium from aqueous solution using poly cyclotriphosphazene co polyethyleneimine microspheres. *J Radioanal Nucl Chem* 326(3):1867–1877
 27. Ma Z, Wang Y, Liu M, Luo Y, Xie X (2019) Highly efficient uranium(VI) removal from aqueous solution using poly(cyclotriphosphazene-co-4,4'-diaminodiphenylether) crosslinked microspheres. *J Radioanal Nucl Chem* 321(3):1093–1107
 28. Sun Y, Kang Y, Zhong W, Liu Y, Dai Y (2020) A simple phosphorylation modification of hydrothermally cross-linked chitosan for selective and efficient removal of U(VI). *J Solid State Chem* 292:121731
 29. Cai Y, Chen L, Yang S, Xu L, Qin HB, Liu Z, Chen L, Wang X, Wang S (2019) Rational synthesis of novel phosphorylated chitosan-carboxymethyl cellulose composite for highly effective decontamination of U(VI). *ACS Sustain Chem Eng* 7(5):5393–5403
 30. Huang Z, Li Z, Zheng L, Zhou L, Chai Z, Wang X, Shi W (2017) Interaction mechanism of uranium(VI) with three-dimensional graphene oxide-chitosan composite: insights from batch experiments, IR, XPS, and EXAFS spectroscopy. *Chem Eng J* 328:1066–1074
 31. Shehzad H, Zhou L, Li Z, Chen Q, Wang Y, Liu Z, Adesina AA (2018) Effective adsorption of U(VI) from aqueous solution using magnetic chitosan nanoparticles grafted with maleic anhydride: equilibrium, kinetic and thermodynamic studies. *J Radioanal Nucl Chem* 315(2):195–206
 32. Fu M, Gao G, Han Y, Lu X, Li J (2020) Adsorption properties of magnetic cross-linked chitosan microspheres to Cu²⁺. *Chem Res Appl* 32(4):664–670
 33. He Y, Wang Y, Zhao W, Gao Y, Lv D (2016) Preparation of magnetic nano-composite adsorbents and their application in water treatment. *Industrial Water Treatment*. 1–10.
 34. Yuan F, Ren W, Huang H (2020) Research progress in the treatment of domestic and industrial wastewater with modified chitosan. *Shangdong Chem Ind* 49(15):75–76
 35. Xu L, Huang Y, Zhu Q, Ye C (2016) Preparation and application of molecularly imprinted polymers based on chitosan. *Chem Ind Eng Progress* 35(3):847–855
 36. Yuan Y, Qian B, Ling X (2019) Modification research progress and application of chitosan. *J Text Sci Eng* 36:81–88
 37. Liu Q, Yu X, Jing Y, Xia W (2012) A comparative study on decoloration properties of two stains by cross-linked chitosan. *J Hebei Univ Technol* 41(5):61–66
 38. Feng Z, Zhao S, Yuan S, Song X, Liang C, Liu F (2018) Adsorption performance of crosslinked chitosan microspheres modified with poly(ethyleneimine) to methyl orange. *Polym Mater Sci Eng* 34:88–93
 39. Yue R, Chen H, Huang Y, Feng P (2019) Cr(VI) removal from water with polyethyleneimine-modified magnetic chitosan. *J Southwest Univ* 41(7):125–130
 40. Zhu W, Dang Q, Liu C, Yu D, Cha D (2019) Cr(VI) and Pb(II) capture on pH-responsive polyethyleneimine and chloroacetic acid functionalized chitosan microspheres. *Carbohydr Polym* 219:353–367
 41. Sun G, Zhou L, Tang X, Le Z, Huang G (2020) In situ formed magnetic chitosan nanoparticles functionalized with polyethyleneimine for effective U(VI) sorption. *J Radioanal Nucl Chem* 325(2):595–604
 42. Chatterjee S, Chatterjee T, Woo SH (2011) Influence of the polyethyleneimine grafting on the adsorption capacity of chitosan beads for reactive black 5 from aqueous solutions. *Chem Eng J* 166(1):168–175
 43. Stopa L, Yamaura M (2010) Uranium removal by chitosan impregnated with magnetite nanoparticles: adsorption and desorption. *Int J Nucl Energy Sci Technol* 5(4):283–289
 44. Zhuang S, Cheng R, Kang M, Wang J (2018) Kinetic and equilibrium of U(VI) adsorption onto magnetic amidoxime-functionalized chitosan beads. *J Clean Prod* 188:655–661
 45. Wang G, Liu J, Wang X, Xie Z, Deng N (2009) Adsorption of uranium(VI) from aqueous solution onto cross-linked chitosan. *J Hazard Mater* 168(2–3):1053–1058
 46. Yang A, Yang P, Huang C (2017) Preparation of graphene oxide-chitosan composite and adsorption performance for uranium. *J Radioanal Nucl Chem* 313(2):371–378
 47. Chen G, Wang H, Han L, Yang N, Hu B, Qiu M, Zhong X (2020) Highly efficient removal of U(VI) by a novel biochar supported with Fe₃O₄ nanoparticles and chitosan composites. *J Mol Liq* 327:114807
 48. Ouyang J, Wang Y, Li T, Zhou L, Liu Z (2018) Immobilization of carboxyl-modified multiwalled carbon nanotubes in chitosan-based composite membranes for U(VI) sorption. *J Radioanal Nucl Chem* 317(3):1419–1428

Publisher's Note Springer Nature remains neutral with regard to jurisdictional claims in published maps and institutional affiliations.